From Asymptotic Freedom to θ Vacua: Qubit Embeddings of the O(3) Nonlinear σ Model

Stephan Caspar* and Hersh Singh†
InQubator for Quantum Simulation (IQuS), Department of Physics, University of Washington, Seattle, Washington 98195-1550, USA

(Received 21 April 2022; accepted 13 June 2022; published 6 July 2022)

Conventional lattice formulations of θ vacua in the $1+1$-dimensional O(3) nonlinear sigma model suffer from a sign problem. Here, we construct the first sign-problem-free regularization for *arbitrary* θ. Using efficient lattice Monte Carlo algorithms, we demonstrate how a Hamiltonian model of spin-$\frac{1}{2}$ degrees of freedom on a two-dimensional spatial lattice reproduces both the infrared sector for arbitrary θ, as well as the ultraviolet physics of asymptotic freedom. Furthermore, as a model of qubits on a two-dimensional square lattice with only nearest-neighbor interactions, it is naturally suited for studying the physics of θ vacua and asymptotic freedom on near-term quantum devices. Our construction generalizes to θ vacua in all $\mathrm{CP}(N-1)$ models, solving a long-standing sign problem.

DOI: 10.1103/PhysRevLett.129.022003

Introduction.—The strong interactions of the standard model described by quantum chromodynamics (QCD) pose a challenging problem for classical computation. While nonperturbative lattice Monte Carlo (MC) methods are a powerful tool for studying static properties of strongly coupled quantum field theories (QFTs) like QCD [1–4], questions involving real-time dynamics, finite density, or nontrivial θ vacua are still out of reach for lattice MC methods due to severe sign problems [5,6].

Emerging quantum platforms provide an exciting possibility for investigating QFTs in previously inaccessible regimes. They are not directly affected by the sign problems arising in classical lattice MC methods. However, bosonic lattice field theories such as QCD have infinite-dimensional local Hilbert spaces, while hardware degrees of freedom (d.o.f.) are usually finite dimensional, mostly qubits. A significant effort is underway to explore different embeddings of QFTs in qubits, with a multitude of ideas emerging from bosonic field theory [7–10], nonlinear sigma models (NLσMs) [11–22], and gauge theories [23–40].

The $1+1$-dimensional O(3) NLσM has a long history as a prototype for QCD, due to similarities such as asymptotic freedom, dynamical transmutation, and the generation of a nonperturbative mass gap, as well as a topological θ term. The O(3) NLσM with a θ term is formally defined by the continuum action

$$S_\theta[\vec{\phi}] = \frac{1}{g^2}\int d^2x(\partial_\mu\vec{\phi})^2 + i\theta Q[\vec{\phi}], \tag{1}$$

where $\vec{\phi}\in\mathbb{R}^3$ with $|\vec{\phi}|^2 = 1$, and

$$Q[\vec{\phi}] = \frac{1}{8\pi}\int d^2x\,\varepsilon_{\mu\nu}\vec{\phi}\cdot(\partial^\mu\vec{\phi})\times(\partial^\nu\vec{\phi}) \tag{2}$$

is the integer topological charge, making the theory 2π periodic in θ. Both $\theta = 0, \pi$ points are well understood, analytically as well as on the lattice. Exact S matrices have been conjectured for both $\theta = 0$ and $\theta = \pi$ [41–44], and their integrability has been confirmed using nonperturbative lattice MC methods [45–47].

However, general, nonintegrable θ remain challenging. It is believed that S_θ for each θ describes a unique asymptotically-free QFT (see Fig. 1). As a topological

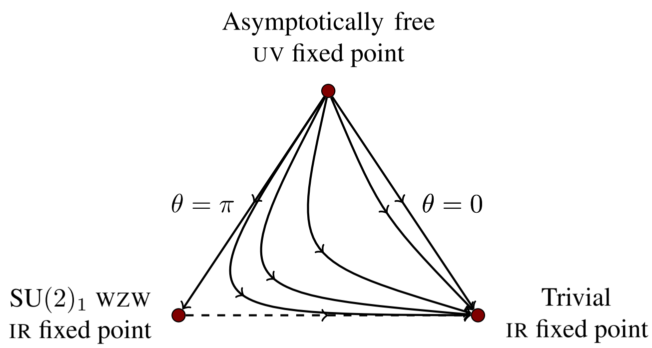

FIG. 1. RG flow diagram of O(3) NLσMs S_θ, defined in Eq. (1). S_θ is a family of asymptotically free QFTs which all flow into the trivial IR fixed point, except at $\theta = \pi$ where it reaches the $\mathrm{SU}(2)_1$ WZW fixed point. At small $|\theta - \pi|$, the RG flow of S_θ passes arbitrarily close to the WZW fixed point, on its way to the trivial fixed point.

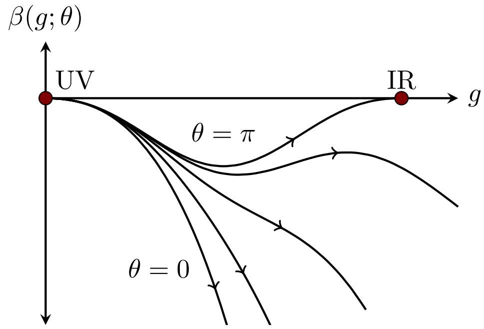

FIG. 2. Qualitative behavior of the β function for the O(3) NLσM at various θ. The zero at $g = 0$ corresponds to the free UV fixed point. At $\theta = \pi$, the β function has an additional fixed point in the IR, corresponding to the $SU(2)_1$ WZW theory. At intermediate θ, the β function $\beta(g;\theta)$ is expected to interpolate between these two curves [49].

effect, θ cannot be studied directly in perturbation theory about the free UV fixed point, but affects the IR physics at strong coupling, as illustrated by the β functions shown in Fig. 2. Nevertheless, some analytic progress has been made by perturbing about the $\theta = \pi$ integrable point [48]. Nonperturbatively, the inclusion of a θ term causes a sign problem when discretizing the action in Eq. (1) on a two-dimensional spacetime lattice. Even though improved actions combined with cluster algorithms have been shown to tame both cutoff effects and the sign problem to allow a reliable extrapolation from modest volumes around $\theta \approx 0$ [49,50], and even fully solve the sign problem at $\theta = \pi$ [46], so far there are no known lattice MC methods which allow a fully controlled study of arbitrary θ vacua.

Motivated by the prospect of quantum simulation to address these challenges, we develop an embedding of the O(3) NLσM at *arbitrary* θ into a two-dimensional Heisenberg antiferromagnet, such that a controlled continuum limit can be taken. Remarkably, not only does this model allow the systematic study of θ vacua on quantum hardware, it also enables the first sign-problem-free algorithm for classical computations at arbitrary θ. This extends similar proposals put forward in Refs. [11,12,14,23] for the classical and quantum simulation of $\theta = 0, \pi$ theories.

Regularizing QFTs using explicitly finite-dimensional local d.o.f. is a promising approach for quantum simulation. Universality lets us understand this remarkable variety in models with the ability to describe the same continuum QFTs. In his seminal work on RG, Wilson showed how continuum QFTs emerge at second-order critical points of lattice models [51–53]. In this framework, the infinite-dimensional continuum fields can arise naturally at long distances from finite-dimensional microscopic local d.o.f. While this approach is natural in the context of quantum computation, universality has even been leveraged to circumvent sign problems that plague conventional lattice regularizations. This was shown, for example, with the O(3) model at finite density [11] and the CP(2) model at $\theta = \pi$ [54]. Efficient cluster algorithms for CP$(N-1)$ models have been demonstrated [13], where a no-go theorem prevents efficient cluster algorithms using the standard lattice action [55].

The qubit Hamiltonian.—In this Letter, we show that the continuum limit of the $1+1$-dimensional O(3) NLσM with a θ term can be obtained from a spin-$\frac{1}{2}$ Heisenberg antiferromagnet on a two-dimensional lattice with staggered couplings

$$H = \sum_{(x,y)} J_{x,y} \vec{S}_{x,y} \cdot \vec{S}_{x+1,y} + J' \sum_{(x,y)} \vec{S}_{x,y} \cdot \vec{S}_{x,y+1}, \qquad (3)$$

where $\vec{S}_i$ are the spin operators acting on two-dimensional Hilbert space at the site (x, y), $J_{x,y}$ are the couplings along the x direction, J' is the coupling along the y direction, and the two-dimensional lattice has dimensions $L_X \times L_Y$. We consider the following two configurations for staggering the couplings:

$$\begin{aligned} &\text{Alternating: } J' > 0, \qquad J_{x,y} = J[1 + (-1)^{x+y}\gamma], \\ &\text{Columnar: } J' < 0, \qquad J_{x,y} = J[1 + (-1)^{x}\gamma], \end{aligned} \qquad (4)$$

where $J > 0$ is always antiferromagnetic, and γ is the staggering parameter, as shown in Fig. 3. In both these cases, the continuum limit of the O(3) NLσM with a θ term can be obtained from odd or even L_Y, by taking the limit $L_Y \to \infty$ at fixed γL_Y such that $L_X \gg L_Y \gg 1$ is maintained.

To demonstrate the continuum limit, we need to recover the physics of the theory described by Eq. (1) at all scales, from the UV to the IR. For all θ, the continuum action S_θ, defined in Eq. (1), describes an asymptotically free theory, controlled in the UV by the fixed point of two free bosons. The coupling g is a relevant coupling and thus drives the theory away from the free UV fixed point into a strongly coupled theory in the IR. While all S_θ theories flow out of the same UV fixed point, nonperturbative effects lead to different RG trajectories for different θ. Figure 1 shows a conjectured RG flow diagram for the O(3) NLσM at

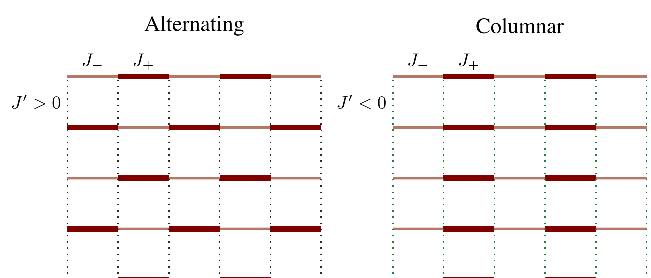

FIG. 3. Two configurations for the staggered interactions, described in Eq. (4), considered as a regularization of the $1+1$-dimensional O(3) NLσM with a θ term. For the alternating staggering, all couplings are antiferromagnetic, while for the columnar case, the transverse coupling J' is ferromagnetic and $J_\pm = J(1 \pm \gamma)$ is antiferromagnetic. All interactions are of the Heisenberg $\vec{S}_i \cdot \vec{S}_j$ type.

arbitrary $0 \leq \theta \leq \pi$, and the corresponding β function is shown in Fig. 2. For all $\theta \neq \pi$ the theory flows to the trivial massive fixed point in the IR. However, at $\theta = \pi$, the theory undergoes a second-order phase transition and the low-energy physics changes completely. The mass gap vanishes, and the IR physics is described by a nontrivial conformal field theory called the $\mathrm{SU}(2)_1$ Wess-Zumino-Witten (WZW) theory [56]. Interestingly, the two ideas of staggering [57,58] and D theory [12] can be combined with the qubit Hamiltonian of Eq. (3) to reproduce the physics of both IR and UV.

IR physics of the θ vacua.—For $\gamma = 0$, the Hamiltonian of Eq. (3) reduces to the ordinary Heisenberg antiferromagnet. For a fixed L_Y and $\gamma = 0$, this model has been studied in condensed matter literature as spin ladders, and is known to be described by the O(3) NLσM at low energies with $\theta = 2\pi S L_Y$ [59–61]. Under this identification, the translation-by-one symmetry of spins ($\vec{S}_{x,y} \mapsto \vec{S}_{x+1,y}$) on the lattice scale becomes the charge conjugation symmetry ($\vec{\phi} \mapsto -\vec{\phi}$) in the continuum. Therefore, a θ term can be induced in the IR by introducing a staggered coupling which breaks this symmetry [57,58,62]. Reference [58] showed that for spin-S ladders with alternating staggering $\theta = 2\pi S L_Y[1 + \gamma f(L_Y)]$, where $f(L_Y)$ is a nonuniversal function. Therefore the low-energy physics of the θ vacua can be studied by varying the staggering parameter γ [63]. However, to obtain the continuum limit of the O(3) NLσM, we must also obtain the physics of asymptotic freedom in the UV, which we now turn to.

Regulating the UV physics and asymptotic freedom.—The continuum limit of S_θ, in Eq. (1), can be obtained from this Hamiltonian model by considering the limit $L_Y \to \infty$ while maintaining $L_X \gg L_Y \gg 1$. This approach has been developed under the name D theory [11,12,23], and works as follows. In the thermodynamic limit $L_X, L_Y \to \infty$, the ground state of the Heisenberg antiferromagnet has Nel ordering with spontaneously broken global SU(2) symmetry, with massless Goldstone mode excitations and diverging correlation length ξ. Now, at finite L_Y, if the correlation length $\xi(L_Y)$ remains larger than L_Y, the system effectively becomes one dimensional. In this regime, the dimensionally reduced system is described by the $1+1$-dimensional O(3) NLσM with an effective coupling $g^2 \sim 1/L_Y$. Due to asymptotic freedom in the $1+1$-dimensional model, the system develops an exponentially large correlation length $\xi \sim e^{\alpha L_Y}$, for some constant α. This guarantees $\xi \gg L_Y$ as L_Y is made larger and confirms the dimensional reduction scenario [11,12,23]. Crucially, since the correlation length diverges with L_Y, a continuum QFT can be defined in the limit of L_Y large. Therefore, in this limit, the spin-$\frac{1}{2}$ Hamiltonian of Eq. (3) is a lattice regularization of the O(3) NLσM with an arbitrary θ at all scales, including asymptotic freedom in the UV.

Extension to $\mathrm{CP}(N-1)$ *models.*—All methods in this Letter are straightforward to extend from $\mathrm{O}(3) = \mathrm{CP}(1)$ to the entire family of $\mathrm{CP}(N-1)$ models, which also allow for a θ term. Both $\theta = 0, \pi$ have been considered before in the D theory formulation [13–15,54] using a Heisenberg model of $\mathrm{SU}(N)$ spins, where the $\mathrm{SU}(N)$ representations are chosen such that spontaneous symmetry breaking of the type $\mathrm{SU}(N) \to \mathrm{U}(N-1)$ occurs [64,65]. This ensures that the continuum $\mathrm{CP}(N-1)$ fields arise as Goldstone modes as the continuum limit ($L_Y \to \infty$) is taken. Since the discussion of charge conjugation symmetry is identical to that for the O(3) model, the staggering patterns of Eq. (4) will induce $\theta \neq 0, \pi$ in these constructions as well.

Methods.—In this Letter, we study the Hamiltonian defined in Eq. (3) by performing MC sampling of the partition function $Z = \mathrm{Tr} e^{-\beta H}$ using a worm algorithm [66–68] on a spacetime lattice at a finite inverse temperature β. The dimensions $L_X \times L_Y$ of the two-dimensional spatial lattices were varied in the range $32 \leq L_X \leq 1024$ and $L_Y = 3,\ 5,\ 7$, with periodic boundary conditions in L_X and open boundary conditions in L_Y. (We choose open boundary conditions in L_Y to avoid frustration.) The couplings $J = |J'| = 1$ were held fixed, and only the staggering γ was varied in the range $0 \leq \gamma L_Y \leq 2$. The Heisenberg model with this level of staggering is not frustrated, and no sign problem occurs in the MC sampling [69,70]. In our computations, the imaginary-time extent β was also discretized into L_T time steps of size ε, such that $\beta = \varepsilon L_T$. Strictly speaking, the Hamiltonian model of Eq. (3) is recovered only by extrapolating to the $\varepsilon \to 0$ limit. Alternatively, one can develop a cluster algorithm directly in the continuous time limit [71]. However, since we are interested in studying the continuum limit of a relativistic field theory, we perform MC computations at a fixed $\varepsilon = 1.0$, which gives a transfer matrix model with the same continuum limit.

For all combinations of the parameters we calculate the second-moment correlation length $\xi_2(L_X, g)$ from the spin-spin correlation function $\langle \vec{S}_{x,y} \cdot \vec{S}_{x',y'} \rangle$. This long distance length scale has been extensively studied at $\theta = 0$ on two-dimensional Euclidean square lattices with the standard action [47,55]. To obtain results for a spacetime symmetric box, we need to tune the imaginary time direction β such that $\beta c = L_X$, where c is the (*a priori* unknown) speed of light. This is achieved by performing computations at a range of β and interpolating to the point where the spatial and temporal second-moment correlation lengths are equal. The calculation is then repeated with doubled volume $2L_X$ but fixed bare couplings $g_{\mathrm{bare}} = (L_Y, J', J, \gamma)$. This macroscopic change in scale $L_X \to 2L_X$ defines a discrete variant of the β function, known as the step-scaling function [45]

$$F_\xi(z) = \frac{\xi_2(2L_X, g_{\mathrm{bare}})}{\xi_2(L_X, g_{\mathrm{bare}})}, \qquad z = \xi_2(L_X, g_{\mathrm{bare}})/L_X, \tag{5}$$

where z defines a renormalized coupling. In the continuum limit $\xi_2 \to \infty$, at constant z, the step-scaling function $F_\xi(z)$ becomes a universal function, which uniquely characterizes the corresponding QFT.

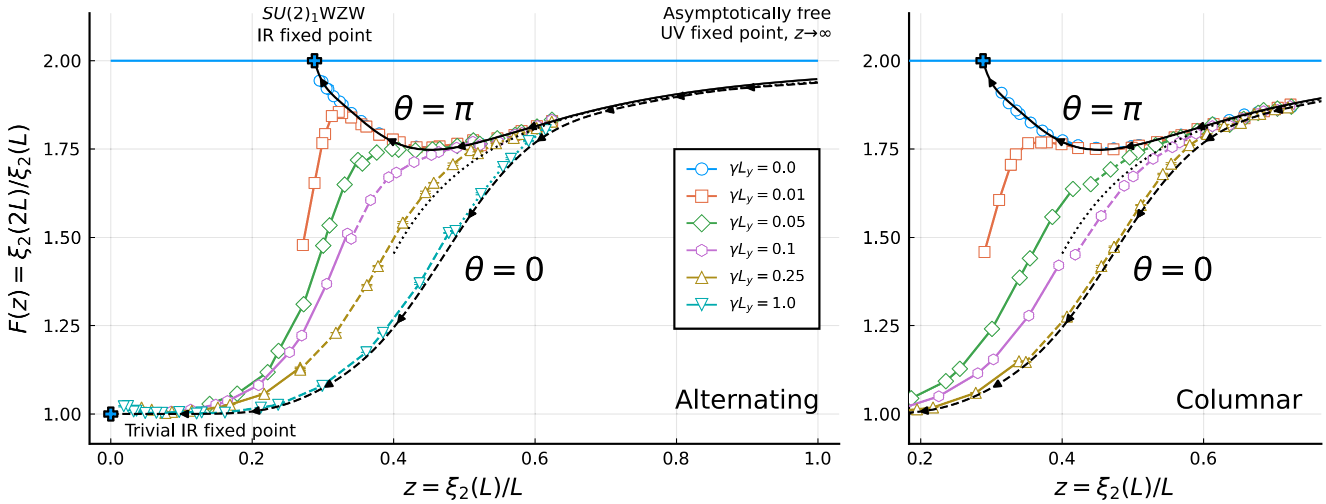

FIG. 4. Step-scaling function of the O(3) NLσM with various θ, as defined in Eq. (5). We show step-scaling curves for different values of $\gamma L_Y \sim |\theta - \pi|/\pi$ with odd L_Y, obtained from alternating (left) and columnar staggering (right), as defined in Eq. (4). For a fixed γL_Y, we show MC results for $L_Y = 3$ (solid line), $L_Y = 5$ (dashed lines), and $L_Y = 7$ (dotted lines). The dotted black curve is a two-loop perturbative prediction [47]. The dashed black line is the step-scaling function for $\theta = 0$ obtained in Ref. [47]. The solid black line is an $O(z^{-10})$ fit to the $\gamma L_Y = 0$ data, which corresponds to the step-scaling function of the O(3) NLσM at $\theta = \pi$. These curves mimic the RG flow diagram shown in Fig. 1, and arrows on the $\theta = 0, \pi$ curves indicate RG flow from UV to IR. All curves agree in the perturbative UV regime, while nonperturbative effects from the θ term lead to divergent trajectories in the IR.

Results.—Figure 4 shows numerical results for the step-scaling function for the O(3) NLσM at various θ, computed using the qubit Hamiltonian of Eq. (3). The results from both alternating (left panel) and columnar (right panel) staggering configurations are shown. To guide the reader, we show three continuous curves: the perturbative prediction (dotted line) and nonperturbative MC results for $\theta = 0$ (black dashed line), and $\theta = \pi$ (black solid line). The perturbative curve is a two-loop computation [47] valid in the UV ($z \gg 1$) and shows asymptotic freedom near the UV fixed point $F(z) = 2$ at $z \to \infty$. The $\theta = 0$ curve was obtained with the standard lattice action in Ref. [47], and shows the flow from the UV to the trivial IR fixed point [$F_\xi(0) = 1$ at $z = 0$].

The $\theta = \pi$ curve (black solid line) is a polynomial fit in z^{-2n} up to order $n = 5$ to our MC results with $\gamma L_Y = 0$. This shows the RG flow from the asymptotically free UV fixed point at $z = \infty$ to the $\mathrm{SU}(2)_1$ WZW fixed point in the IR at $z = z^*$. We estimate the location of the nontrivial IR fixed point to be $z^* \approx 0.28$ where $F(z^*) = 2$, which is the discrete equivalent of a vanishing β function. We emphasize that the physics of *all* scales, from asymptotic freedom in the UV to the $\mathrm{SU}(2)_1$ WZW theory in the IR, is reproduced by this model.

The remaining curves show new results for nonzero $\gamma L_Y \sim |\theta - \pi|/\pi$. The $\theta = 0, \pi$ curves form a lower and upper bound on all step-scaling curves $0 \le \theta \le \pi$. All curves closely follow the perturbative two-loop calculation (dotted line) at large z down to $z \approx 0.75$. At lower values of the renormalized coupling, nonperturbative effects start to dominate, leading to divergent trajectories.

For small staggering γL_Y the curves closely track the $\theta = \pi$ curve. But since θ is a relevant perturbation about the WZW fixed point, the RG trajectories cannot reach the nontrivial fixed point at z^* and ultimately have to flow away to the trivial fixed point at $z = 0$, consistent with the fact that these theories are massive. These theories can be made to pass arbitrarily close to the $\mathrm{SU}(2)_1$ WZW fixed point by choosing smaller and smaller γL_Y, without the need for any fine tuning, exemplified by the curve $\gamma L_Y = 0.01$ in Fig. 4. This is the phenomenon of conformal walking, which is also exhibited by QCD-like four-dimensional non-Abelian gauge theories near the conformal window [72], or technicolor extensions of the standard model [49,73].

As the staggering γ is increased further, the step-scaling curves trace out the entire area bounded by the two curves $\theta = 0, \pi$, demonstrating that all θ vacua are contained in this model. However, this only yields a qualitative relationship between γL_Y and θ. Semiclassical results from large-(SL_Y) expansions [58,74] suggest that the relationship should be linear, $\theta = 2\pi S L_Y[1 + \gamma f(L_Y)]$ with $f(L_Y) \to f(\infty)$ approaching a finite constant in the large-L_Y limit. Numerically, we observe that a value of $\gamma L_Y = 1.0$ ($\gamma L_Y = 0.25$) approximates the $\theta = 0$ curve with the alternating (columnar) staggering. Additional data also show a periodic reappearance of $\theta = \pi$ around values of $\gamma L_Y = 2.0$ ($\gamma L_Y = 0.5$). From this we estimate the asymptotic values $f(\infty) \approx 1.0$ for alternating and $f(\infty) \approx 0.25$ for columnar staggering. The small discontinuities of the step-scaling curves between different values of $L_Y = 3$, 5, 7 suggest that the corrections to $f(L_Y)$ at finite L_Y are mild, especially considering that similar values of the renormalized coupling $z = \xi_2(L_X, g)/L_X$ were obtained with drastically different lattice spacings (usually $L_X = 64$ for the smaller L_Y compared with $L_X = 1024$ for the larger L_Y).

Similar results are also observed with even ladders, where the staggering γ is a perturbation about the $\theta = 0$ theory. Preliminary results from $L_Y = 2, 4, 6$ with alternating and columnar staggerings suggest that $\theta = \pi$ can also be obtained in this way. These results strongly motivate a conjecture: the continuum limit ($L_Y \to \infty$, with L_Y either odd or even) for each fixed γL_Y is in fact a *unique* QFT corresponding to the $1+1$-dimensional O(3) NLσM with a fixed θ,

$$\theta \equiv \pi L_Y(1 + \gamma f) \pmod{2\pi}, \tag{6}$$

where f is a nonuniversal constant which depends on the details of the model such as choice of couplings, staggering configuration, and whether L_Y is odd or even. While we have provided strong evidence in favor of the identification in Eq. (6), there are many paths forward to establish this more rigorously. For example, odd and even L_Y could be used to self-validate this conjecture, by showing that their step-scaling functions agree by appropriately tuning γL_Y. Further, a comparison with the approach of Ref. [50] using topological lattice actions would be very illuminating. In that approach, θ appears as a manifestly topological parameter and thus does not require an empirical identification like Eq. (6). Any universal quantity computable in both regularizations would allow the matching of θ with γL_Y, for example, $F(z)$ at a single fixed value of z. Topological quantities such as susceptibilities and instanton distributions have long been known to be divergent in the O(3) model [73,75–78]. How these issues manifest in the qubit Hamiltonian setup would be very interesting to clarify.

Conclusions.—In this Letter, we have shown how to implement the $1+1$-dimensional O(3) NLσM at arbitrary θ using qubit degrees of freedom. While the motivation behind this work is the quantum simulation of θ vacua on near-term quantum hardware, interestingly, this result also advances lattice computations of QFTs using *classical* MC methods. On the classical side, it provides the first sign-problem-free MC algorithm for arbitrary θ. Our numerical results, obtained with an efficient worm algorithm, indicate that the entire range of θ vacua is contained in this model, and we conjecture a simple prescription of how the continuum limit can be reached and the physics at all scales can be studied.

This construction enables real-time simulation of θ vacua in the O(3) NLσM on near-term quantum hardware. These theories can be regularized at any lattice spacing through an embedding into a two-dimensional square lattice of qubits with nearest-neighbor Heisenberg-type interactions. The alternating staggering is a prime candidate for an analog quantum simulation platform like ultracold atoms, with uniform pairwise interactions, and couplings that can be arranged through the trapping pattern shown in Fig. 5. On digital quantum hardware like superconducting qubits or trapped ions, either staggering can be implemented using standard Suzuki-Trotter decompositions. For example, it was shown in Ref. [79] that each trotterized nearest-neighbor Heisenberg interaction $e^{i\epsilon J_{xy}\vec{S}_x\cdot\vec{S}_y}$ can be implemented using just three CNOT gates. Interestingly, the limit $L_X \gg L_Y$ is also amenable to tensor network algorithms, which would be powerful complementary approach to lattice MC and quantum simulation going forward.

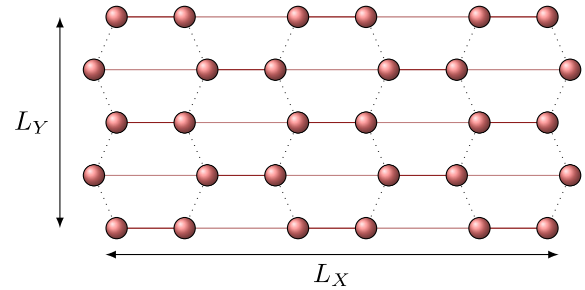

FIG. 5. Proposed embedding of the O(3) NLσM with a θ term into a two-dimensional array of ultracold atoms. The alternating staggering described in Eq. (4) and Fig. 3 arises naturally from distance-dependent antiferromagnetic interactions by deforming a rectangular lattice.

In lattice field theory, the $1+1$-dimensional O(3) NLσM has been long considered an ideal testbed for static properties of QCD, exhibiting many of its features, including asymptotic freedom and θ vacua. Even more possibilities open up once we have access to real-time dynamics using quantum platforms. For instance, accessing nontrivial θ would allow the study of inelastic scattering processes in an asymptotically free theory, which would have been impossible in the integrable $\theta = 0, \pi$ theories.

Formulating QFTs using qubits can yield unexpected advantages. For the O(3) NLσM, this approach has the rather remarkable feature that it completely circumvents a sign problem present in conventional lattice formulations of the θ term, and is amenable to efficient cluster algorithms. Extension to the entire family of CP$(N-1)$ models is straightforward. This is encouraging on the path forward toward studying QCD with novel classical and quantum algorithms. Our results demonstrate that there is no fundamental obstruction to studying θ vacua with discrete degrees of freedom, but whether such ideas might one day even help with the sign problems in QCD remains to be seen.

We learned about D theory from Shailesh Chandrasekharan and Uwe-Jens Wiese and are grateful to them for many enlightening conversations over the years. We thank Martin Savage for inspiring discussions and important feedback on the manuscript. We would also like to acknowledge stimulating conversations with Tanmoy Bhattacharya, Anthony Ciavarella, Daniel Nogradi, Mendel Nguyen, and Mithat Ünsal on related matters.

The material presented here was funded in part by the DOE QuantISED program through the theory consortium "Intersections of QIS and Theoretical Particle Physics" at Fermilab with Fermilab Subcontract No. 666484, in part by the Institute for Nuclear Theory with US Department of Energy Grant No. DE-FG02-00ER41132, and in part by the U.S. Department of Energy, Office of Science, Office of Nuclear Physics, InQubator for Quantum Simulation (IQuS) under Award No. DOE (NP) DE-SC0020970.

*caspar@uw.edu
†hershsg@uw.edu

[1] C. Ratti, Lattice QCD and heavy ion collisions: A review of recent progress, Rep. Prog. Phys. **81**, 084301 (2018).
[2] Z. Davoudi, W. Detmold, P. Shanahan, K. Orginos, A. Parreño, M. J. Savage, and M. L. Wagman, Nuclear matrix elements from lattice QCD for electroweak and beyond-Standard-Model processes, Phys. Rep. **900**, 1 (2021).
[3] M. T. Hansen and S. R. Sharpe, Lattice QCD and three-particle decays of resonances, Annu. Rev. Nucl. Part. Sci. **69**, 65 (2019).
[4] M. Constantinou *et al.*, Parton distributions and lattice-QCD calculations: Toward 3D structure, Prog. Part. Nucl. Phys. **121**, 103908 (2021).
[5] S. D. Hsu and D. Reeb, On the sign problem in dense QCD, Int. J. Mod. Phys. A **25**, 53 (2010).
[6] V. Goy, V. Bornyakov, D. Boyda, A. Molochkov, A. Nakamura, A. Nikolaev, and V. Zakharov, Sign problem in finite density lattice QCD, Prog. Theor. Exp. Phys. **2017**, 031D01 (2017).
[7] S. P. Jordan, K. S. Lee, and J. Preskill, Quantum computation of scattering in scalar quantum field theories, Quantum Inf. Comput. **14**, 1014 (2014).
[8] S. P. Jordan, K. S. Lee, and J. Preskill, Quantum algorithms for quantum field theories, Science **336**, 1130 (2012).
[9] K. Yeter-Aydeniz, E. F. Dumitrescu, A. J. McCaskey, R. S. Bennink, R. C. Pooser, and G. Siopsis, Scalar quantum field theories as a benchmark for near-term quantum computers, Phys. Rev. A **99**, 032306 (2019).
[10] N. Klco and M. J. Savage, Digitization of scalar fields for quantum computing, Phys. Rev. A **99**, 052335 (2019).
[11] S. Chandrasekharan, B. Scarlet, and U. J. Wiese, From spin ladders to the 2D O(3) model at non-zero density, Comput. Phys. Commun. **147**, 388 (2002).
[12] R. Brower, S. Chandrasekharan, S. Riederer, and U. J. Wiese, D-theory: Field quantization by dimensional reduction of discrete variables, Nucl. Phys. **B693**, 149 (2004).
[13] B. B. Beard, M. Pepe, S. Riederer, and U.-J. Wiese, Efficient cluster algorithm for CP$(N-1)$ models, Comput. Phys. Commun. **175**, 629 (2006).
[14] C. Laflamme, W. Evans, M. Dalmonte, U. Gerber, H. Mejía-Díaz, W. Bietenholz, U. J. Wiese, and P. Zoller, CP(N-1) quantum field theories with alkaline-earth atoms in optical lattices, Ann. Phys. (Amsterdam) **370**, 117 (2016).
[15] W. Evans, U. Gerber, M. Hornung, and U. J. Wiese, $SU(3)$ quantum spin ladders as a regularization of the CP(2) model at non-zero density: From classical to quantum simulation, Ann. Phys. (Amsterdam) **398**, 94 (2018).
[16] F. Bruckmann, K. Jansen, and S. Kühn, $O(3)$ nonlinear sigma model in $1+1$ dimensions with matrix product states, Phys. Rev. D **99**, 074501 (2019).
[17] H. Singh and S. Chandrasekharan, A qubit regularization of the $O(3)$ sigma model, Phys. Rev. D **100**, 054505 (2019).
[18] T. Bhattacharya, A. J. Buser, S. Chandrasekharan, R. Gupta, and H. Singh, Qubit Regularization of Asymptotic Freedom, Phys. Rev. Lett. **126**, 172001 (2021).
[19] H. Singh, Qubit $O(N)$ nonlinear sigma models, Phys. Rev. D **105**, 114509 (2022).
[20] H. Singh, Large-charge conformal dimensions at the $O(N)$ Wilson-Fisher fixed point, arXiv:2203.00059.
[21] A. Alexandru, P. F. Bedaque, H. Lamm, and S. Lawrence, Sigma Models on Quantum Computers, Phys. Rev. Lett. **123**, 090501 (2019).
[22] A. Alexandru, P. F. Bedaque, A. Carosso, and A. Sheng, Universality of a truncated sigma-model, arXiv:2109.07500.
[23] S. Chandrasekharan and U. J. Wiese, Quantum link models: A discrete approach to gauge theories, Nucl. Phys. **B492**, 455 (1997).
[24] R. Brower, S. Chandrasekharan, and U. J. Wiese, QCD as a quantum link model, Phys. Rev. D **60**, 094502 (1999).
[25] I. Raychowdhury and J. R. Stryker, Solving Gauss's law on digital quantum computers with loop-string-hadron digitization, Phys. Rev. Research **2**, 033039 (2020).
[26] R. Anishetty, M. Mathur, and I. Raychowdhury, Prepotential formulation of SU(3) lattice gauge theory, J. Phys. A **43**, 035403 (2010).
[27] D. Banerjee, M. Bögli, M. Dalmonte, E. Rico, P. Stebler, U.-J. Wiese, and P. Zoller, Atomic Quantum Simulation of U(N) and SU(N) Non-Abelian Lattice Gauge Theories, Phys. Rev. Lett. **110**, 125303 (2013).
[28] E. Zohar, J. I. Cirac, and B. Reznik, Quantum simulations of lattice gauge theories using ultracold atoms in optical lattices, Rep. Prog. Phys. **79**, 014401 (2016).
[29] M. C. Banuls, K. Cichy, J. I. Cirac, K. Jansen, and S. Kühn, Efficient Basis Formulation for $(1+1)$-Dimensional SU(2) Lattice Gauge Theory: Spectral Calculations with Matrix Product States, Phys. Rev. X **7**, 041046 (2017).
[30] C. Muschik, M. Heyl, E. Martinez, T. Monz, P. Schindler, B. Vogell, M. Dalmonte, P. Hauke, R. Blatt, and P. Zoller, U(1) Wilson lattice gauge theories in digital quantum simulators, New J. Phys. **19**, 103020 (2017).
[31] T. V. Zache, F. Hebenstreit, F. Jendrzejewski, M. Oberthaler, J. Berges, and P. Hauke, Quantum simulation of lattice gauge theories using Wilson fermions, Quantum Sci. Technol. **3**, 034010 (2018).
[32] A. Alexandru, P. F. Bedaque, S. Harmalkar, H. Lamm, S. Lawrence, and N. C. Warrington (NuQS Collaboration), Gluon field digitization for quantum computers, Phys. Rev. D **100**, 114501 (2019).
[33] J. Bender and E. Zohar, Gauge redundancy-free formulation of compact QED with dynamical matter for quantum and classical computations, Phys. Rev. D **102**, 114517 (2020).

[34] Z. Davoudi, M. Hafezi, C. Monroe, G. Pagano, A. Seif, and A. Shaw, Towards analog quantum simulations of lattice gauge theories with trapped ions, Phys. Rev. Research **2**, 023015 (2020).

[35] N. Klco, M. J. Savage, and J. R. Stryker, SU(2) non-Abelian gauge field theory in one dimension on digital quantum computers, Phys. Rev. D **101**, 074512 (2020).

[36] A. F. Shaw, P. Lougovski, J. R. Stryker, and N. Wiebe, Quantum algorithms for simulating the lattice Schwinger model, Quantum **4**, 306 (2020).

[37] V. Kasper, T. V. Zache, F. Jendrzejewski, M. Lewenstein, and E. Zohar, Non-Abelian gauge invariance from dynamical decoupling, arXiv:2012.08620.

[38] A. J. Buser, H. Gharibyan, M. Hanada, M. Honda, and J. Liu, Quantum simulation of gauge theory via orbifold lattice, J. High Energy Phys. 09 (2021) (034).

[39] J. F. Haase, L. Dellantonio, A. Celi, D. Paulson, A. Kan, K. Jansen, and C. A. Muschik, A resource efficient approach for quantum and classical simulations of gauge theories in particle physics, Quantum **5**, 393 (2021).

[40] A. Alexandru, P. F. Bedaque, R. Brett, and H. Lamm, Spectrum of digitized QCD: Glueballs in a $S(1080)$ gauge theory, Phys. Rev. D **105**, 114508 (2022).

[41] A. B. Zamolodchikov and A. B. Zamolodchikov, Factorized S-matrices in two dimensions as the exact solutions of certain relativistic quantum field theory models, Ann. Phys. (N.Y.) **120**, 253 (1979).

[42] J. Balog and Á. Hegedűs, TBA equations for excited states in the O(3) and O(4) nonlinear-model, J. Phys. A **37**, 1881 (2004).

[43] J. Balog and Á. Hegedűs, The finite size spectrum of the 2-dimensional O(3) nonlinear σ-model, Nucl. Phys. **B829**, 425 (2010).

[44] M. Lüscher, Quantum non-local charges and absence of particle production in the two-dimensional non-linear σ-model, Nucl. Phys. **B135**, 1 (1978).

[45] M. Lüscher, P. Weisz, and U. Wolff, A numerical method to compute the running coupling in asymptotically free theories, Nucl. Phys. **B359**, 221 (1991).

[46] W. Bietenholz, A. Pochinsky, and U.-J. Wiese, Testing Haldane's conjecture in the O(3) model by a Meron cluster simulation, Nucl. Phys. B, Proc. Suppl. **47**, 727 (1996).

[47] S. Caracciolo, R. G. Edwards, A. Pelissetto, and A. D. Sokal, Asymptotic Scaling in the Two-Dimensional O(3) σ Model at Correlation Length 10^5, Phys. Rev. Lett. **75**, 1891 (1995).

[48] J. Balog, P. Forgacs, and L. Palla, A two-dimensional integrable axionic sigma-model and T-duality, Phys. Lett. B **484**, 367 (2000).

[49] P. de Forcrand, M. Pepe, and U. J. Wiese, Walking near a conformal fixed point: The 2-d $o(3)$ model at $\theta \approx \pi$ as a test case, Phys. Rev. D **86**, 075006 (2012).

[50] M. Bogli, F. Niedermayer, M. Pepe, and U. J. Wiese, Non-trivial θ-vacuum effects in the 2-d o(3) model, J. High Energy Phys. 04 (2012) 117.

[51] K. G. Wilson and J. B. Kogut, The renormalization group and the epsilon expansion, Phys. Rep. **12**, 75 (1974).

[52] K. G. Wilson, The renormalization group and critical phenomena, Rev. Mod. Phys. **55**, 583 (1983).

[53] J. B. Kogut, An introduction to lattice gauge theory and spin systems, Rev. Mod. Phys. **51**, 659 (1979).

[54] B. B. Beard, M. Pepe, S. Riederer, and U.-J. Wiese, Study of $\mathrm{CP}(n-1)$ θ-Vacua by Cluster Simulation of $\mathrm{SU}(n)$ Quantum Spin Ladders, Phys. Rev. Lett. **94**, 010603 (2005).

[55] S. Caracciolo, R. G. Edwards, A. Pelissetto, and A. D. Sokal, Wolff type embedding algorithms for general nonlinear sigma models, Nucl. Phys. **B403**, 475 (1993).

[56] R. Shankar and N. Read, The $\vartheta = \pi$ nonlinear sigma model is massless, Nucl. Phys. **B336**, 457 (1990).

[57] I. Affleck, Field theory methods and quantum critical phenomena, in *Les Houches Summer School in Theoretical Physics: Fields, Strings, Critical Phenomena* (1988), https://inspirehep.net/literature/265102.

[58] M. A. Martín-Delgado, R. Shankar, and G. Sierra, Phase Transitions in Staggered Spin Ladders, Phys. Rev. Lett. **77**, 3443 (1996).

[59] G. Sierra, The nonlinear sigma model and spin ladders, J. Phys. A **29**, 3299 (1996).

[60] F. D. M. Haldane, Continuum dynamics of the 1-D Heisenberg antiferromagnetic identification with the O(3) nonlinear sigma model, Phys. Lett. A **93**, 464 (1983).

[61] F. D. M. Haldane, Nonlinear Field Theory of Large Spin Heisenberg Antiferromagnets. Semiclassically Quantized Solitons of the One-Dimensional Easy Axis Neel State, Phys. Rev. Lett. **50**, 1153 (1983).

[62] I. Affleck and F. D. M. Haldane, Critical theory of quantum spin chains, Phys. Rev. B **36**, 5291 (1987).

[63] L. C. Venuti, C. D. E. Boschi, E. Ercolessi, F. Ortolani, G. Morandi, S. Pasini, and M. Roncaglia, Particle content of the nonlinear sigma model with a θ-term: A lattice model investigation, J. Stat. Mech. (2005) L02004.

[64] N. Read and S. Sachdev, Valence-Bond and Spin-Peierls Ground Sates of Low-Dimensional Quantum Antiferromagnets, Phys. Rev. Lett. **62**, 1694 (1989).

[65] N. Read and S. Sachdev, Some features of the phase diagram of the square lattice SU(N) antiferromagnet, Nucl. Phys. **B316**, 609 (1989).

[66] N. Prokof'ev and B. Svistunov, Worm algorithm for problems of quantum and classical statistics, arXiv:0910.1393.

[67] N. Prokof'ev and B. Svistunov, Worm Algorithms for Classical Statistical Models, Phys. Rev. Lett. **87**, 160601 (2001).

[68] U. J. Wiese and H. P. Ying, A determination of the low energy parameters of the 2-d Heisenberg antiferromagnet, Z. Phys. B **93**, 147 (1994).

[69] H. G. Evertz, The loop algorithm, Adv. Phys. **52**, 1 (2003).

[70] O. F. Syljuåsen and A. W. Sandvik, Quantum Monte Carlo with directed loops, Phys. Rev. E **66**, 046701 (2002).

[71] B. B. Beard and U.-J. Wiese, Simulations of Discrete Quantum Systems in Continuous Euclidean Time, Phys. Rev. Lett. **77**, 5130 (1996).

[72] T. Banks and A. Zaks, On the phase structure of vector-like gauge theories with massless fermions, Nucl. Phys. **B196**, 189 (1982).

[73] D. Nogradi, An ideal toy model for confining, walking and conformal gauge theories: The O(3) sigma model with theta-term, J. High Energy Phys. 05 (2012) 089.

[74] G. Sierra, On the application of the nonlinear sigma model to spin chains and spin ladders, Lect. Notes Phys. **478**, 137 (1997).

[75] B. Berg and M. Lüscher, Definition and statistical distributions of a topological number in the lattice O(3) σ-model, Nucl. Phys. **B190**, 412 (1981).

[76] W. Bietenholz, J. C. P. Barros, S. Caspar, M. Hornung, and U.-J. Wiese, Meron- and semi-vortex-clusters as physical carriers of topological charge and vorticity, Proc. Sci., LATTICE2019 (**2019**) 288.

[77] P. Schwab, Two-instanton contribution to the topological susceptibility in CP^{n-1}-models on a sphere, Phys. Lett. **126B**, 241 (1983).

[78] P. Schwab, Semiclassical approximation for the topological susceptibility in CP^{n-1}-models on a sphere, Phys. Lett. **118B**, 373 (1982).

[79] G. Vidal and C. M. Dawson, Universal quantum circuit for two-qubit transformations with three controlled-NOT gates, Phys. Rev. A **69**, 010301(R) (2004).